catalysts

MDPI

Article

In Situ XRD Study on Stability and Performance of Co_3C Catalyst in Fischer–Tropsch Synthesis

Xianfeng Shen [1,2,3,*,†], Xiao Han [2,3,4,†], Tianfu Zhang [5], Haiyun Suo [3], Lai Yan [3], Ming Qing [3], Yi He [1], Yongwang Li [2,3] and Yong Yang [2,3,*]

1 College of Chemical and Biological Engineering, Zhejiang University, Hangzhou 310027, China; yihe@zju-qz.edu.cn
2 State Key Laboratory of Coal Conversion, Institute of Coal Chemistry, Chinese Academy of Sciences, Taiyuan 030001, China; hanxiao19@mails.ucas.ac.cn (X.H.); ywl@sxicc.ac.cn (Y.L.)
3 National Energy Center for Coal to Liquids, Synfuels China Co., Ltd., Huairou District, Beijing 101407, China; suohaiyun@synfuelschina.com.cn (H.S.); yanlai@synfuelschina.com.cn (L.Y.); qingming@synfuelschina.com.cn (M.Q.)
4 University of Chinese Academy of Sciences, Beijing 100049, China
5 Carbon Neutrality Research Center, State Power Investment Corporation Research Institute, Changping District, Beijing 102299, China; zhangtianfu@spic.com.cn
* Correspondence: shenxianfeng@zju.edu.cn (X.S.); yyong@sxicc.ac.cn (Y.Y.)
† These authors contributed equally to this work.

Abstract: Cobalt carbides have been recognized as an active phase for the production of light olefins and alcohols in Fischer–Tropsch synthesis. In this study, in situ X-ray diffraction experiments were performed to investigate the stability and catalytic performance over a single-phase Co_3C catalyst under reaction conditions. The in situ X-ray diffraction results indicated that the Co_3C phase remained stable with no significant changes until the temperature reached 300 °C. The high stability can be attributed to the twinning structure of the single-phase Co_3C catalyst. The catalytic evaluation results showed that the single-phase Co_3C catalyst had higher activity with high selectivity to long-chain products due to the unique surface structure of Co_3C. This work provides guidance for the rational design of efficient cobalt carbide catalysts for Fischer–Tropsch synthesis reactions.

Keywords: Fischer–Tropsch synthesis; Co_3C; stability; in situ XRD

Citation: Shen, X.; Han, X.; Zhang, T.; Suo, H.; Yan, L.; Qing, M.; He, Y.; Li, Y.; Yang, Y. In Situ XRD Study on Stability and Performance of Co_3C Catalyst in Fischer–Tropsch Synthesis. *Catalysts* **2024**, *14*, 483. https://doi.org/10.3390/catal14080483

Academic Editor: Maria A. Goula

Received: 16 July 2024
Revised: 25 July 2024
Accepted: 26 July 2024
Published: 28 July 2024

1. Introduction

Due to environmental pollution and the decrease in crude oil feeds, scientists have researched new routes to produce clean liquid fuels and chemicals from renewable feedstocks [1,2]. Fischer–Tropsch synthesis (FTS) is one of the most effective pathways to produce clean fuels, such as gasoline, diesel, paraffin and so on, through the catalytic conversion of the syngas (CO + H_2) derived from coal, biomass and natural gas [3–5]. The catalytic performance of FTS catalysts is closely related to the catalyst properties. Among these catalysts, Fe- and Co-based catalysts are commonly applied in commercial plants [3,6,7]. Compared with Fe-based catalysts, there are lots of advantages of Co-based catalysts, such as high activity, moderate price, low water gas shift activity and high selectivity for heavy hydrocarbons [3,8–10].

Generally, metallic Co is considered as the active phase in the Co-based FTS process [9,11,12]. However, bulk cobalt carbides (Co_2C/Co_3C) can form during the FTS process under a lean H_2 atmosphere. In previous reports, cobalt carbides were an inactive phase in FTS. Claeys et al. [13] revealed that Co_2C decomposed to metallic Co in argon at 300 °C by an in situ magnetometer, which resulted in the recovery of activity. Although cobalt carbide shows poor performance in FTS, several studies have reported that it exhibits high catalytic activity for the synthesis of oxygenates and olefins. Zhong et al. [14,15] proposed that specific facets of Co_2C nanoprisms were responsible for the formation of

olefins. Furthermore, Ding et al. [16–18] claimed that the interface between cobalt/cobalt carbide provides active sites for oxygenates in syngas conversion due to the dual sites for CO insertion into hydrocarbons for oxygenates.

In addition to Co_2C catalysts, another form of cobalt carbide, Co_3C, also plays a vital role in the production of lower olefins during the FTS reaction. Recently, Liu [19,20] and his colleagues found that metallic Co(111) transformed into Co_3C(101), which exhibited a high selectivity to light olefins. By utilizing density functional theory (DFT) calculations, they proposed that Co_3C(101) is beneficial for C-C coupling under the synergistic effect between the unique surface structure and electronic properties. Recently, we reported on a Co-based catalyst with different phase structures for different carburization times [21,22]. The catalysts with the Co/Co_3C phase exhibited higher catalytic activity, as compared with metallic Co catalysts and Co/Co_2C catalysts. Combining with the experimental and theoretical results, we revealed that Co_3C can activate CO more easily than Co and Co_2C, which leads to excellent catalytic performance during the FTS reaction. However, most previous studies mainly focused on hybrid phase Co_3C catalysts (Co/Co_3C) [19–21]. To the best of our knowledge, the FTS reaction over single-phase Co_3C catalysts has never been investigated. Moreover, the stability of the Co_3C catalyst under FTS conditions is also rarely reported on.

In this study, we synthesized a single-phase Co_3C (S-Co_3C) catalyst by using the wet chemical method. Various characterization techniques were used to study the morphology, phase composition and particle size of the catalyst. Subsequently, in situ X-ray diffraction (in situ XRD) was used to detect the phase changes in the Co_3C catalyst under FTS reaction conditions. The Co_3C catalyst remained stable and did not decompose when the reaction temperature increased to 300 °C. The Co_3C catalyst exhibited excellent catalytic performance, achieving a 27% CO conversion and a 78.5% C_{5+} selectivity at 300 °C. This work has further enhanced our understanding of the Co_3C catalyst in a Co-based FTS reaction and guided us in the rational design of effective catalysts for the FTS reaction.

2. Results and Discussion

2.1. Characterization of Co_3C Catalyst

Firstly, we used the wet chemistry method to synthesize the S-Co_3C catalyst as reported in our previous study [23]. The XRD pattern of the synthesized S-Co_3C catalyst is presented in Figure S1. The XRD results indicated that the S-Co_3C catalyst can be synthesized. The morphology and structure of the S-Co_3C catalyst were investigated by using SEM and (HR)TEM, as shown in Figure S2. This further suggested that S-Co_3C was successfully synthesized. Considering that the Co_2C catalyst can also influence the catalytic performance during FTS, a single-phase Co_2C (S-Co_2C) catalyst was also prepared and compared. As displayed in Figure S3, all the diffraction peaks can be ascribed to the crystal planes of Co_2C. This indicated that we synthesized the S-Co_2C catalyst by using the wet chemistry method.

2.2. Stability of Co_3C Catalyst

Furthermore, the phase transformation of the S-Co_3C catalyst during the FTS reaction under syngas (H_2/CO = 2) atmosphere at different temperatures was conducted by using in situ XRD. As shown in Figure 1, the initial reaction temperature was 150 °C; all the diffraction peaks can be assigned to Co_3C crystallites. Then, the temperature increased to 200 °C, and no obvious changes were observed. Afterwards, the temperature continuously increased until it reached 300 °C to observe the phase transformation of the catalyst. The phase composition of the catalyst remained unchanged during the reaction. The temperature was decreased to 220 °C and 260 °C (220-R and 260-R) to detect the phase transition in Figure 1, and no changes were observed after the temperature decrease. This suggested that Co_3C crystallites can stably exist and are resistant to the conditions of the FTS reaction, which is consistent with our previous studies [19,21,22].

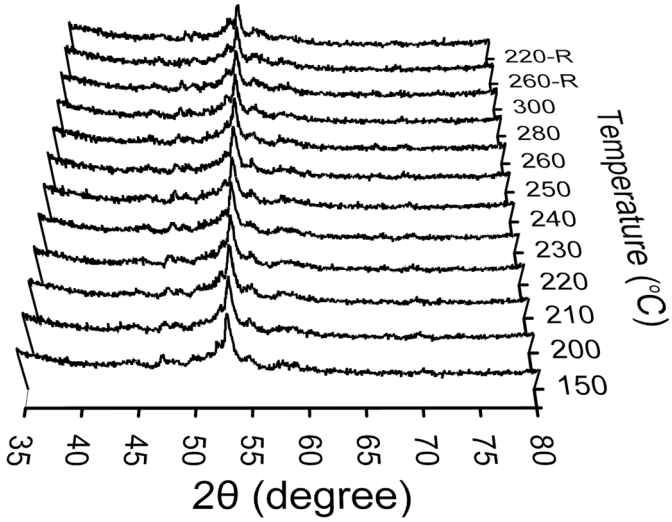

Figure 1. In situ XRD pattern of Co_3C catalyst.

For comparison with the Co_3C catalyst, the phase transformation of the Co_2C catalyst was also observed on in situ XRD shown in Figure 2. The initial reaction temperature was 180 °C, and all the diffraction peaks can be assigned to Co_2C crystallites. Following an increase in the reaction temperature to 240 °C, a transition was observed from Co_2C crystallites to Co crystallites. Afterwards, as the reaction temperature increased, there was a corresponding gradual increase in the diffraction intensity of the Co crystallites. However, the Co_2C crystallites maintained their dominance in the catalyst. The results indicated that the Co_2C catalyst is more unstable compared to the Co_3C catalyst under the syngas atmosphere at high temperature (T > 240 °C).

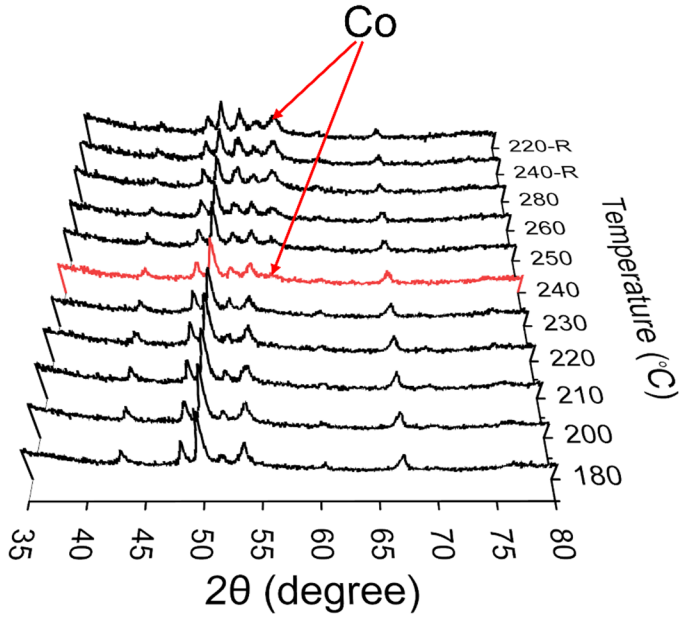

Figure 2. In situ XRD pattern of Co_2C catalyst.

2.3. Catalytic Performance

The S-Co_3C catalyst was evaluated to determine the relationship between phase transformation and catalytic performance, and the reaction condition of $H_2/CO = 2$, 0.2 MPa and GHSV = 25,000 mL g_{cat}^{-1} h^{-1} was applied at different reaction temperatures. As shown in Figure 3a, the S-Co_3C catalyst had no catalytic activity between 150 °C and 240 °C. It is speculated that this may be due to low reaction pressure, less catalyst loading

or high space velocity. When the temperature reached 250 °C, the CO conversion of the S-Co_3C catalyst was 16.1%. After the reaction temperature was raised to 260 °C and 280 °C, the activity exhibited a slight increase with the CO conversion corresponding to 17.8% and 18.4%, respectively. Eventually, the temperature was raised to 300 °C, and the CO conversion reached 27%. The CO conversion was lower at low temperatures compared to higher temperatures. This can be attributed to the absence of adequate energy to activate the reactant on the catalyst at low temperatures. Many researchers have drawn similar conclusions on the effect of temperature on the performance of cobalt catalysts [24–27]. We also evaluated the stability of the S-Co_3C catalyst for a long-term reaction (24 h) in a microreactor under the same reaction conditions. The results are shown in Figure S4; the CO conversion remained consistently stable at approximately 30%. The S-Co_2C catalyst was also evaluated at 180 °C to 280 °C; there is no activity for the FTS reaction, as shown in Table S1. Although metallic Co appeared into the catalyst above 240 °C, its activity is still negligible due to the low content of Co.

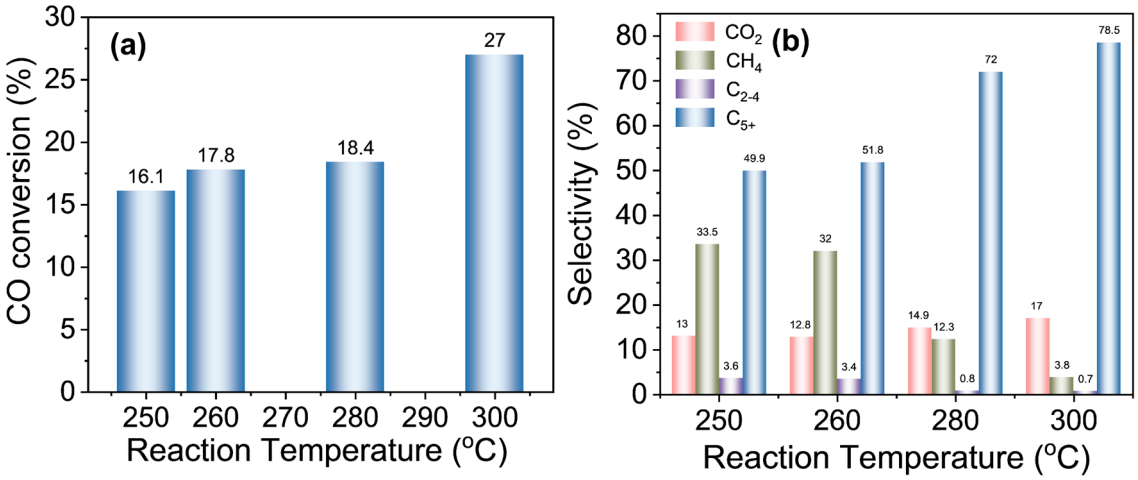

Figure 3. Performance of Co_3C catalyst for FTS. (**a**) CO conversion and (**b**) product distribution at different temperatures. $C_{2–4}$: Hydrocarbons with carbon numbers from 2 to 4. C_{5+}: Hydrocarbons with carbon numbers more than 4. Reaction conditions: H_2/CO = 2; P = 0.2 MPa; GSHV = 25,000 mL g_{cat}^{-1} h^{-1}.

Figure 3b displays the effects of reaction temperature on the product selectivity over the S-Co_3C catalyst. At 250 °C, the catalyst produced about 13% CO_2 and approximately increased to 17% at 300 °C. However, the CH_4 selectivity remained constant at about 33% below 260 °C. At above 260 °C, the CH_4 selectivity dramatically decreased to 12.3% at 280 °C and 3.8% at 300 °C. The selectivity of $C_{2–4}$ products also decreased from 3.6% at 250 °C to 0.7% at 300 °C. For the long-chain products of C_{5+}, the selectivity increased from 49.9% to 78.5%. The C_{5+} selectivity remained constant below 260 °C. While the temperature increased to 280 °C and 300 °C, the C_{5+} selectivity dramatically increased to 72% and 78.5%, respectively. Herein, the S-Co_3C catalyst not only exhibited a higher CO conversion but also had higher C_{5+} selectivity and lower CH_4 selectivity.

2.4. Discussion

The stability of the S-Co_3C catalyst was investigated by in situ XRD measurements. Conventional views have suggested that the Co_2C or Co_3C structure can be easily reduced to metallic Co during the FTS reaction [13,28]. However, more and more recent studies have reported that the Co_2C or Co_3C structure can stably exist as catalysts and exhibit excellent catalytic performance [15,20,29]. In this study, we found that the Co_3C structure was more stable than the Co_2C structure under high temperature conditions. We therefore speculated that the difference in catalyst stability can be attributed to the different atomic arrangements of C and Co atoms. The Co_2C structure can be formed by the diffusion of

surface C atoms into HCP or FCC Co atoms and can be considered as the formation of Ni_2C [30,31]. However, the Co_3C structure has no simple relation to the atomic arrangement in Co atoms. The crystal structure of Co_3C is isomorphous to that of Fe_3C. This means that the Co_3C structure can be visualized as the twinning of HCP-Co cells with C atoms filling interstitial sites [30,32,33]. Comparing the two structures, we can speculate that the C atom lattice interstices are more easily moved out than those in the twinning structure. Therefore, the Co_3C structure is more stable than the Co_2C structure, with a higher decomposition temperature.

Previously, we reported that the catalysts including the Co_3C structure exhibit excellent catalytic performance during the FTS reaction [21,22]. In this study, the CO conversion of the S-Co_3C catalyst reached 27% with a C_{5+} selectivity of 78.5% and a CH_4 selectivity of 3.8% at 300 °C. Under the conditions of high space velocity and low pressure, the S-Co_3C catalyst had very good activity, in line with our previous studies. The results can be attributed to the high intrinsic activity of the Co_3C structure. In our previous theoretical studies, we investigated the activation barrier for CO activation among Co(0001), Co_2C(111) and Co_3C(221). We found that Co_3C(221) was the most active surface for CO activation with the lowest activation barrier. Herein, this work further confirmed the positive role of the Co_3C structure during the FTS reaction.

The effect of reaction temperature on product distribution was also discussed. CO_2 is mainly generated by the water gas shift (WGS) reaction on the Co-based catalysts. As the reaction temperature rose from 250 to 300 °C, the conversion of CO also increased. This led to an increase in water formation, which promoted the formation of CO_2 through the WGS reaction [24,34,35]. Previous studies reported that the selectivity for CH_4 increases and C_{5+} products decrease with the temperature increases on metallic Co catalysts [24,26,34]. This result can be ascribed to the high rates of product desorption and the reduced residence time on the metallic Co catalyst surface at high temperature. However, it was observed that as the temperature increased, the selectivity of CH_4 decreased, and the selectivity of C_{5+} products increased in this study. We speculated that the Co_3C structure may affect the product distribution. In our previous studies, we investigated the effects of the Co_3C structure on olefin oligomerization [36]. We found that the Co_3C structure is more favorable for C-C coupling than that of metallic Co, which can be attributed to the lower position of the d band center of Co_3C(221). This result is consistent with other reports, which demonstrated that the low d band center facilitates C-C coupling [20,37]. Consequently, the high selectivity of long-chain products is attributed to the downward shift of the d band center in the Co_3C catalyst. The experimental results in this work exhibit a significant correlation with our prior theoretical results in the product selectivity trend. It can be concluded that the Co_3C catalyst is beneficial for the production of long-chain products while also serving to prevent the formation of methane at high reaction temperatures.

3. Experimental Section

3.1. Reagents

Cobalt acetate tetrahydrate, Polyethylene glycol 200 (PEG-200), Glucose and Potassium Hydroxide (KOH) were purchased from Sinopharm chemical Reagent Co. Ltd., Shanghai, China, without further purification. Tetraethylene glycol (TEG) was purchased from Alfa and used without further purification.

3.2. Catalyst Preparation

Preparation of Co_3C catalyst [23]: A total of 1 mmol cobalt acetate tetrahydrate and 1 mmol glucose were added to 60 mL TEG to form a solution in a 100 mL four-necked flask. Subsequently, the temperature was raised to 290 °C (1 °C/min) and refluxed for 180 min in nitrogen atmosphere. After the temperature dropped to room temperature, the solution was washed five times with distilled water and acetone solution to obtain a black solid. Finally, the precipitate was dried at 60 °C for 6 h in a vacuum oven to obtain the Co_3C catalyst.

3.3. Catalyst Characterizations

3.3.1. X-ray Diffraction

The XRD patterns of the catalysts were collected on an X-ray diffractometer (Bruker, Germany) with Co Kα radiation at 35 kV and 40 mA. The scan rate of samples was set at 4.8°/min from 20° to 80°.

3.3.2. Scanning Electron Microscopy and Transmission Electron Microscopy

Scanning electron microscopy (SEM) measurements were performed on a FEI Quanta 400 field-emission scanning electron microscope. Transmission electron microscopy (TEM) images were obtained using a FEI Talos F200A electron microscope at 200 kV accelerating voltage. Before the measurements, the catalyst powder was dispersed in ethanol under sonication for 30 min. The resulting suspended powder was dropped on a copper grid covered with carbon film.

3.3.3. In Situ XRD Experiments

The in situ XRD experiments of the catalysts were conducted to detect the phase transformation during the FTS reaction by using a Bruker D8 Advance XRD equipped with Co Kα radiation at 35 kV and 40 mA. The in situ reaction system was specially designed and supplied by University of Cape Town (UCT) [38].

All the in situ experiments were performed in a capillary with an outside diameter of 1.0 mm, a wall thickness of 0.02 mm and a length of 75 mm. About 20 mg of catalyst was loaded into the capillary. Afterwards, the syngas (H_2/CO = 2) with a flow rate of 25,000 mL $g_{cat}{}^{-1}$ h^{-1} was introduced into the system. The reaction temperature was ramped to 150 °C to collect spectra; the same procedure was repeated at 180 °C, 200 °C, 210 °C, 220 °C, 230 °C, 240 °C, 250 °C, 260 °C, 280 °C and 300 °C. The scan rate of samples was set at 4.8°/min from 35°to 80°.

3.4. Catalyst Evolution

FTS reactions were performed on the in situ XRD equipment. The 20 mg catalyst was loaded into the capillary. The FTS reactions were investigated in a stream of syngas (H_2/CO = 2) with a flow rate of 25,000 mL $g_{cat}{}^{-1}$ h^{-1} at 0.2 MPa. The reaction temperature was kept consistent with the temperature used in the in situ XRD experiments. And each temperature was held constant for 30 min to collect detailed data, including CO conversion and product selectivity.

The effluent gas was detected online using Agilent 7890B gas chromatography equipment. H_2, N_2, CO, CH_4 and CO_2 flowed through a column packed with a PLOT Q and 5A molecular sieve, and they were analyzed with a thermal conductivity detector (TCD). The hydrocarbons flowed through a GAS pro column and were analyzed with a flame ionization detector (FID). We used the internal standard method to calculate the CO conversion and product selectivity. For the internal standard, 4% Ar in 64% H_2/32% CO was used for the CO conversion calculation. The selectivity and CO conversion can be calculated using the following formulas:

$$\text{CO Conv.} = \frac{n_{CO,in}/n_{Ar,in} - n_{CO,out}/n_{Ar,out}}{n_{CO,in}/n_{Ar,in}}$$

Selectivity of CH_4:

$$CH_4\ \text{Sel.} = \frac{n_{CH4,out}/n_{Ar,out}}{n_{CO,in}/n_{Ar,in} - n_{CO,out}/n_{Ar,out}}$$

Selectivity of $C_{2–4}$:

$$C_{x(2–4)}\ \text{Sel.} = \frac{\left[n_{Cx(2–4),out}/n_{Ar,out}\right]\cdot x_{(2–4)}}{n_{CO,in}/n_{Ar,in} - n_{CO,out}/n_{Ar,out}}$$

Selectivity of CO_2:

$$CO_2\ \text{Sel.} = \frac{n_{CO2,out}/n_{Ar,out}}{n_{CO,in}/n_{Ar,in} - n_{CO,out}/n_{Ar,out}}$$

Selectivity of C_{5+}:

$$C_{5+}\ \text{Sel.} = 1 - (CH_4\ \text{Sel.} + C_{2-4}\ \text{Sel.} + CO_2\ \text{Sel.})$$

4. Conclusions

In the present study, we investigated the stability and performance of the Co_3C catalyst in the FTS reaction by using in situ XRD. The S-Co_3C catalyst demonstrated excellent stability at high reaction temperature (<300 °C) under syngas atmosphere. The unique twinning structure results in the carbon atoms being difficult to remove, which is responsible for the high stability at high temperature. The S-Co_3C catalyst exhibited higher activity with a high selectivity of heavy hydrocarbons. The high activity of the catalyst is derived from the high intrinsic activity of the Co_3C structure, which facilitates the CO activation during the FTS reaction. The high selectivity of heavy hydrocarbons can be attributed to the lower position of the d band center of Co_3C. This study sheds new light on the stability of the Co_3C catalyst and presents a reasonable route for designing highly active cobalt carbide catalysts for the FTS reaction.

Supplementary Materials: The following supporting information can be downloaded at: https://www.mdpi.com/article/10.3390/catal14080483/s1. Figure S1: XRD pattern of Co_3C catalyst; Figure S2: (a) SEM image, (b) TEM image, (c) HRTEM image, and (d) FFT image of (c) image of Co_3C catalyst; Figure S3. XRD pattern of Co_2C catalyst [39]; Figure S4: CO conversion of Co_3C catalyst as a function of time on stream; Table S1: The catalytic performance over Co_2C catalyst for FT synthesis at different temperature.

Author Contributions: Conceptualization, X.S., T.Z. and Y.Y.; methodology, X.S.; software, Y.H.; validation, X.S. and X.H.; formal analysis, X.S. and X.H.; investigation, X.S., T.Z. and Y.Y.; resources, Y.Y. and Y.L.; data curation, X.S., X.H. and L.Y.; writing—original draft preparation, X.S. and X.H.; writing—review and editing, X.S., Y.Y., T.Z., L.Y. and H.S.; visualization, M.Q.; supervision, Y.Y. and Y.L.; project administration, Y.Y. and Y.L.; funding acquisition, Y.Y. and Y.L. All authors have read and agreed to the published version of the manuscript.

Funding: This research was funded by the National Science Fund for Distinguished Young Scholars for Yong Yang grant number 22025804, the National Key Research and Development Program of China for Yi He grant number 2022YFE0106100 and the National Natural Science Foundation of China for Yi He grant number 22178299. And the APC was funded by Xianfeng Shen.

Data Availability Statement: The original contributions presented in the study are included in the article (and Supplementary Materials), further inquiries can be directed to the corresponding authors.

Acknowledgments: This work was financially supported by the National Science Fund for Distinguished Young Scholars (Grant No. 22025804), the National Key Research and Development Program of China (Grant No. 2022YFE0106100) and the National Natural Science Foundation of China (Grant No. 22178299). We also thank Synfuels China Co., Ltd. and Beijing Key Laboratory of Coal Cleaning Liquid Fuels.

Conflicts of Interest: Author Xianfeng Shen, Xiao Han, Haiyun Suo, Lai Yan, Ming Qing, Yongwang Li and Yong Yang was employed by the company National Energy Center for Coal to Liquids, Synfuels China Co., Ltd. The remaining authors declare that the research was conducted in the absence of any com-mercial or financial relationships that could be construed as a potential conflict of interest.

References

1. Chong, J.W.; Chemmangattuvalappil, N.G.; Thangalazhy-Gopakumar, S. Aviation Biofuels: Conversion Routes and Challenges. In *Sustainable Technologies for the Oil Palm Industry: Latest Advances and Case Studies*; Foo, C.Y.D., Tun Abdul Aziz, M.K., Yusup, S., Eds.; Springer Nature: Singapore, 2023; pp. 33–85.
2. Olah, G.A. Towards oil independence through renewable methanol chemistry. *Angew. Chem. Int. Ed. Engl.* **2013**, *52*, 104–107. [CrossRef] [PubMed]
3. van de Loosdrecht, J.; Botes, F.G.; Ciobica, I.M.; Ferreira, A.; Gibson, P.; Moodley, D.J.; Saib, A.M.; Visagie, J.L.; Weststrate, C.J.; Niemantsverdriet, J.W. Fischer–Tropsch Synthesis: Catalysts and Chemistry. In *Comprehensive Inorganic Chemistry II*; Elsevier: Amsterdam, The Netherlands, 2013; pp. 525–557.
4. Qi, Z.; Chen, L.; Zhang, S.; Su, J.; Somorjai, G.A. A mini review of cobalt-based nanocatalyst in Fischer-Tropsch synthesis. *Appl. Catal. A General.* **2020**, *602*, 117701. [CrossRef]
5. Gholami, Z.; Tišler, Z.; Rubáš, V. Recent advances in Fischer-Tropsch synthesis using cobalt-based catalysts: A review on supports, promoters, and reactors. *Catal. Rev.* **2020**, *63*, 512–595. [CrossRef]
6. Chang, Q.; Zhang, C.; Liu, C.; Wei, Y.; Cheruvathur, A.V.; Dugulan, A.I.; Niemantsverdriet, J.W.; Liu, X.; He, Y.; Qing, M.; et al. Relationship between Iron Carbide Phases (ε-Fe_2C, Fe_7C_3, and χ-Fe_5C_2) and Catalytic Performances of Fe/SiO_2 Fischer–Tropsch Catalysts. *ACS Catal.* **2018**, *8*, 3304–3316. [CrossRef]
7. Yin, J.; Wang, S.; Xu, D.; You, Y.; Liu, X.; Peng, Q. Surface modification of Fe_5C_2 by binding silica-based ligand: A theoretical explanation of enhanced C2 oxygenate selectivity. *Mol. Catal.* **2023**, *547*, 113333. [CrossRef]
8. Li, Z.; Zhong, L.; Yu, F.; An, Y.; Dai, Y.; Yang, Y.; Lin, T.; Li, S.; Wang, H.; Gao, P.; et al. Effects of Sodium on the Catalytic Performance of CoMn Catalysts for Fischer–Tropsch to Olefin Reactions. *ACS Catal.* **2017**, *7*, 3622–3631. [CrossRef]
9. Lyu, S.; Wang, L.; Zhang, J.; Liu, C.; Sun, J.; Peng, B.; Wang, Y.; Rappé, K.G.; Zhang, Y.; Li, J.; et al. Role of Active Phase in Fischer–Tropsch Synthesis: Experimental Evidence of CO Activation over Single-Phase Cobalt Catalysts. *ACS Catal.* **2018**, *8*, 7787–7798. [CrossRef]
10. Qin, C.; Hou, B.; Wang, J.; Wang, Q.; Wang, G.; Yu, M.; Chen, C.; Jia, L.; Li, D. Crystal-Plane-Dependent Fischer–Tropsch Performance of Cobalt Catalysts. *ACS Catal.* **2018**, *8*, 9447–9455. [CrossRef]
11. ten Have, I.C.; Weckhuysen, B.M. The active phase in cobalt-based Fischer-Tropsch synthesis. *Chem. Catal.* **2021**, *1*, 339–363. [CrossRef]
12. Liu, J.-X.; Su, H.-Y.; Sun, D.-P.; Zhang, B.-Y.; Li, W.-X. Crystallographic Dependence of CO Activation on Cobalt Catalysts: HCP versus FCC. *J. Am. Chem. Soc.* **2013**, *135*, 16284–16287. [CrossRef]
13. Claeys, M.; Dry, M.E.; van Steen, E.; du Plessis, E.; van Berge, P.J.; Saib, A.M.; Moodley, D.J. In situ magnetometer study on the formation and stability of cobalt carbide in Fischer–Tropsch synthesis. *J. Catal.* **2014**, *318*, 193–202. [CrossRef]
14. Zhong, L.; Yu, F.; An, Y.; Zhao, Y.; Sun, Y.; Li, Z.; Lin, T.; Lin, Y.; Qi, X.; Dai, Y.; et al. Cobalt carbide nanoprisms for direct production of lower olefins from syngas. *Nature* **2016**, *538*, 84–87. [CrossRef] [PubMed]
15. Lin, T.; Yu, F.; An, Y.; Qin, T.; Li, L.; Gong, K.; Zhong, L.; Sun, Y. Cobalt Carbide Nanocatalysts for Efficient Syngas Conversion to Value-Added Chemicals with High Selectivity. *Acc. Chem. Res.* **2021**, *54*, 1961–1971. [CrossRef] [PubMed]
16. Pei, Y.-P.; Liu, J.-X.; Zhao, Y.-H.; Ding, Y.-J.; Liu, T.; Dong, W.-D.; Zhu, H.-J.; Su, H.-Y.; Yan, L.; Li, J.-L.; et al. High Alcohols Synthesis via Fischer-Tropsch Reaction at Cobalt Metal/Carbide Interface. *ACS Catal.* **2015**, *5*, 3620–3624. [CrossRef]
17. Pei, Y.; Ding, Y.; Zhu, H.; Du, H. One-step production of C1-C18 alcohols via Fischer-Tropsch reaction over activated carbon-supported cobalt catalysts: Promotional effect of modification by SiO_2. *Chin. J. Catal.* **2015**, *36*, 355–361. [CrossRef]
18. Zhao, Z.; Lu, W.; Yang, R.; Zhu, H.; Dong, W.; Sun, F.; Jiang, Z.; Lyu, Y.; Liu, T.; Du, H.; et al. Insight into the formation of $Co@Co_2C$ catalysts for direct synthesis of higher alcohols and olefins from syngas. *ACS Catal.* **2017**, *8*, 228–241. [CrossRef]
19. Zheng, J.; Cai, J.; Jiang, F.; Xu, Y.; Liu, X. Investigation of the highly tunable selectivity to linear α-olefins in Fischer-Tropsch synthesis over silica-supported Co and CoMn catalysts by carburization-reduction pretreatment. *Catal. Sci. Technol.* **2017**, *7*, 4736–4755. [CrossRef]
20. Liu, B.; Li, W.; Xu, Y.; Lin, Q.; Jiang, F.; Liu, X. Insight into the Intrinsic Active Site for Selective Production of Light Olefins in Cobalt-Catalyzed Fischer–Tropsch Synthesis. *ACS Catal.* **2019**, *9*, 7073–7089. [CrossRef]
21. Shen, X.; Luo, D.; Ma, C.; Suo, H.; Yan, L.; Zhang, T.; Liu, X.; Wen, X.; Li, Y.; Yang, Y. Carburized cobalt catalyst for the Fischer–Tropsch synthesis. *Catal. Sci. Technol.* **2021**, *11*, 6564–6572. [CrossRef]
22. Shen, X.; Han, X.; Zhang, T.; Suo, H.; Yan, L.; Li, Y.; Yang, Y. Effects of Co_3C formation on the catalytic performance for Fischer-Tropsch synthesis over Co/SiO_2 catalysts. *Mol. Catal.* **2024**, *555*, 113889. [CrossRef]
23. Shen, X.; Ma, C.; Suo, H.; Zhang, T.; Yan, L.; Huang, L.; Zhou, J.; Wen, X.; Li, Y.; Yang, Y. Wet-chemistry approach for the synthesis of single phase ferromagnetic Co_3C nanoparticle. *Nano Sel.* **2021**, *2*, 1368–1371. [CrossRef]
24. Ghogia, A.C.; Nzihou, A.; Serp, P.; Soulantica, K.; Pham Minh, D. Cobalt catalysts on carbon-based materials for Fischer-Tropsch synthesis: A review. *Appl. Catal. A Gen.* **2021**, *609*, 117906. [CrossRef]
25. Rashed, A.E.; Nasser, A.; Elkady, M.F.; Matsushita, Y.; Abd El-Moneim, A. Temperature calibration effect on FTS activity and product selectivity using Fe-MOF catalyst. *Case Stud. Chem. Environ. Eng.* **2023**, *7*, 100300. [CrossRef]
26. Honsho, T.-o.; Kitano, T.; Miyake, T.; Suzuki, T. Fischer–Tropsch synthesis over Co-loaded oxidized diamond catalyst. *Fuel* **2012**, *94*, 170–177. [CrossRef]

27. Nohtani, R.; Mirzaei, A.A.; Eshraghi, A. Synthesis of Fe–Co–Ce/Zeolite A-3 Catalysts and their Selectivity to Light Olefins for Fischer–Tropsch Synthesis in Fixed-Bed Reactor. *Catal. Lett.* **2019**, *149*, 522–532. [CrossRef]
28. Kwak, G.; Kim, D.-E.; Kim, Y.T.; Park, H.-G.; Kang, S.C.; Ha, K.-S.; Jun, K.-W.; Lee, Y.-J. Enhanced catalytic activity of cobalt catalysts for Fischer–Tropsch synthesis via carburization and hydrogenation and its application to regeneration. *Catal. Sci. Technol.* **2016**, *6*, 4594–4600. [CrossRef]
29. Dong, W.; Liu, J.; Zhu, H.; Ding, Y.; Pei, Y.; Liu, J.; Du, H.; Jiang, M.; Liu, T.; Su, H.; et al. Co–Co_2C and Co–Co_2C/AC Catalysts for Hydroformylation of 1-Hexene under Low Pressure: Experimental and Theoretical Studies. *J. Phys. Chem. C* **2014**, *118*, 19114–19122. [CrossRef]
30. Carroll, K.J.; Huba, Z.J.; Spurgeon, S.R.; Carpenter, E. Magnetic properties of Co_2C and Co_3C nanoparticles and their assemblies. *Appl. Phys. Lett.* **2012**, *101*, 012409. [CrossRef]
31. Stolbov, S.; Hong, S.; Kara, A.; Rahman, T.S. Origin of the C-inducedp4greconstruction of Ni(001). *Phys. Rev. B* **2005**, *72*, 155423. [CrossRef]
32. Wood, I.G.; Vočadlo, L.; Knight, K.S.; Dobson, D.P.; Marshall, W.G.; Price, G.D.; Brodholt, J. Thermal expansion and crystal structure of cementite, Fe_3C, between 4 and 600 K determined by time-of-flight neutron powder diffraction. *J. Appl. Crystallogr.* **2004**, *37*, 82–90. [CrossRef]
33. Shein, I.R.; Medvedeva, N.I.; Ivanovskii, A.L. Electronic and structural properties of cementite-type M_3X (M = Fe, Co, Ni; X = C or B) by first principles calculations. *Phys. B Condens. Matter* **2006**, *371*, 126–132. [CrossRef]
34. Aluha, J.; Gutierrez, S.; Gitzhofer, F.; Abatzoglou, N. Use of Plasma-Synthesized Nano-Catalysts for CO Hydrogenation in Low-Temperature Fischer(-)Tropsch Synthesis: Effect of Catalyst Pre-Treatment. *Nanomaterials* **2018**, *8*, 822. [CrossRef] [PubMed]
35. Pendyala, V.R.R.; Shafer, W.D.; Jacobs, G.; Davis, B.H. Fischer–Tropsch Synthesis: Effect of Reaction Temperature for Aqueous-Phase Synthesis Over a Platinum Promoted Co/Alumina Catalyst. *Catal. Lett.* **2014**, *144*, 1088–1095. [CrossRef]
36. Shen, X.; Luo, D.; Ni, J.; Wu, J.; Ma, C.; Suo, H.; Liu, X.; Lv, Z.; Wen, X.; Li, Y.; et al. The effect of surface carbon on ethylene dimerization. *Appl. Surf. Sci.* **2021**, *570*, 151210. [CrossRef]
37. Zhang, R.; Wen, G.; Adidharma, H.; Russell, A.G.; Wang, B.; Radosz, M.; Fan, M. C_2 Oxygenate Synthesis via Fischer–Tropsch Synthesis on Co_2C and Co/Co_2C Interface Catalysts: How to Control the Catalyst Crystal Facet for Optimal Selectivity. *ACS Catal.* **2017**, *7*, 8285–8295. [CrossRef]
38. Niu, L.; Liu, X.; Liu, X.; Lv, Z.; Zhang, C.; Wen, X.; Yang, Y.; Li, Y.; Xu, J. In Situ XRD Study on Promotional Effect of Potassium on Carburization of Spray-dried Precipitated Fe_2O_3 Catalysts. *ChemCatChem* **2017**, *9*, 1691–1700. [CrossRef]
39. Shen, X.; Zhang, T.; Suo, H.; Yan, L.; Huang, L.; Ma, C.; Li, L.; Wen, X.; Li, Y.; Yang, Y. A facile one-pot method for synthesis of single phase Co_2C with magnetic properties. *Mater. Lett.* **2020**, *271*, 127783. [CrossRef]